

볼트 체결된 대형 상용차 프레임의 응력해석

김진곤† · 박용국*

(원고접수일 : 2003년 2월 21일, 심사완료일 : 2003년 7월 3일)

Stress Analysis of Large Commercial Vehicle Frames with Bolted Joints

Jin-Gon Kim† · Yong-Kuk Park*

Abstract : Structural failures, such as crack initiation, often arise near the bolted parts of the side member and trunnion bracket in some commercial vehicles. The purpose of this paper is: 1) establishment of a simple and practical bolted joint modelling technique and 2) determination of the key design variables for design improvement based on numerical experiments. Once the bolted joint modelling technique is established through experimental verification, the key design variables must be identified in order to alleviate the level of the stress concentration near the problem region. Numerical results indicate that the torsional rigidity of the frame cross-section should be increased to reduce the level of the maximum stress at the actual crack initiation location.

Key words : Stress analysis, Commercial vehicle frame, Bolted joints, Crack initiation, Design variable

1. Introduction

Near the bolted parts of the side frame and trunnion bracket of some commercial vehicles shown in Fig. 1, some problems, such as crack initiation often arise after some years in service. The trunnion bracket is the vehicle component which allows load distributions between two

pairs of rear wheels. If designers cannot predict the stress level near the bolted joints of the structures, the structural failures may not be prevented. Although commercial finite element software packages can be used to achieve this goal, it is still a demanding task to model bolted parts. Special elements like gap elements may be used, but one may not

† Corresponding author, School of Mech. and Auto. Eng., Catholic University of Daegu

* School of Mech. and Auto. Eng., Catholic University of Daegu,
E-mail: ykpark@cu.ac.kr, T : 053)850-2723

obtain converging results despite of a substantial amount of CPU time. Even after a reliable modelling technique is successfully established, design variables must be carefully selected for future design improvement.

This research work serves two major purposes. The first is mainly focused on the establishment of a simple and practical bolted joint modelling technique. The second is the determination of the key design variables. As far as bolted joint modelling techniques are concerned, there are many studies to determine the joint stiffness in bolted connections through detailed finite element modelling or experiments⁽¹⁾⁻⁽³⁾. However, the detailed modelling may be too complex to use in the prediction of the stress level in complex structures. One objective of the present work is to find a practical and reliable bolted joint modelling technique that does not require special elements. Thus several modelling techniques are examined, and static and dynamic experiments are also conducted on a simple test model to discover the best modelling technique among those considered.

Stress analysis of a commercial vehicle chassis frame is then conducted under several loading conditions utilizing the selected bolted joint modelling technique. Through the numerical results, the critical design variables in reducing the magnitude of the maximum stress near the bolted joint of the frame and trunnion, are identified to be the torsional rigidity of the frame cross section and the size of the trunnion

bracket. In a situation where the frame cross section cannot be easily modified, resizing of the trunnion bracket will be a practical alternative.

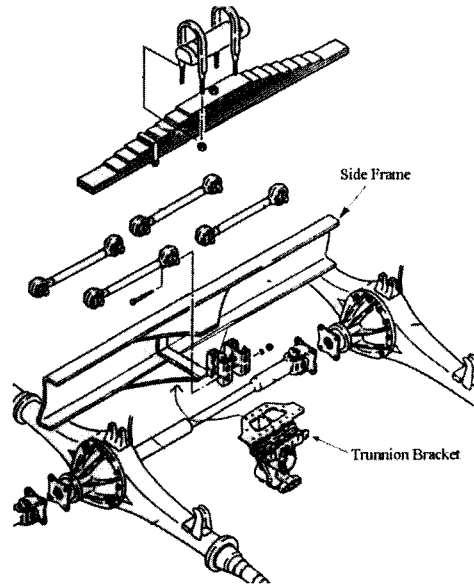


Fig. 1 Trunnion bracket mounting system in the rear wheels

2. Bolted joint modelling and experimental verification

2.1 Modelling of bolted joints

Several modelling techniques of bolted joints are examined in this section. Among various modelling techniques, only those which can be practically used in the industry, are investigated. The neutral surfaces of the joined upper and lower plates by a bolt in Fig. 2 are modelled with plate/shell elements, in which the distance between two plates is denoted by 'a'. Furthermore, the use of special elements such as gap elements is excluded. Special elements are difficult to

use and they do not always yield converging results even with a huge consumption of computational time. The followings are the modelling techniques that are examined in the present work.

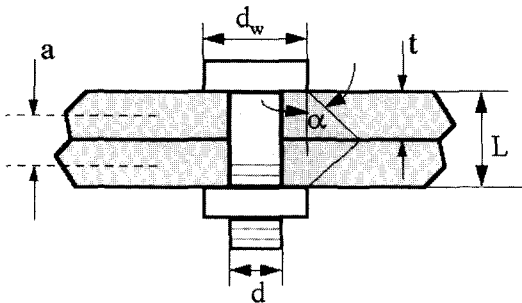


Fig. 2 General bolted joint

2.1.1. Modelling (a)

A bolt is modeled with only one rigid element, which connects one point at each connected plate. The top and bottom of the bolt shank of diameter d is modeled with plate/shell elements. This modelling technique has often been adopted in the automotive industry to predict low-frequency structural behavior. (See Fig. 3(a).)

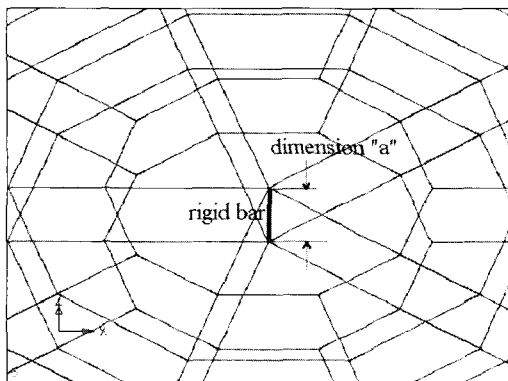


Fig. 3 (a) Modelling (a): One rigid element at the center to connect the upper and lower plates

2.1.2. Modelling (b)

In Modelling (a), in order to account for the stiffness of the joint area, the elastic modulus of the plate/shell elements corresponding to the top and bottom of the bolt shank is increased to be ten times larger than that of the adjacent plates. (See Fig. 3(b).)

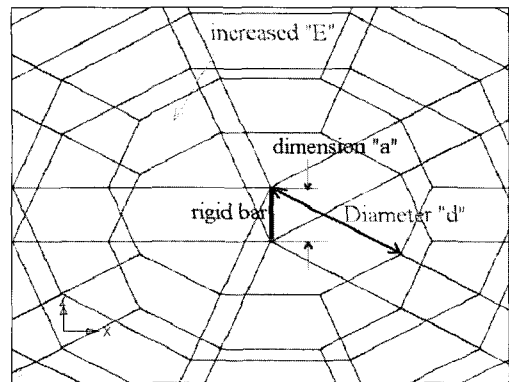


Fig. 3 (b) Modelling (b): One rigid element at the center to connect the upper and lower plates, and the increased elastic modulus of the plate/shell elements corresponding to the top and bottom of the bolt shank

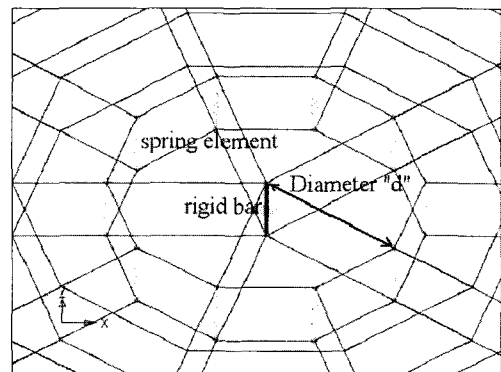


Fig. 3 (c) Modelling (c): One rigid element at the center and spring elements with the stiffness in Equation (2) along the boundary of the bolt shank

2.1.3. Modelling (c)

The bolt connection is modelled with

one rigid element at its center but the boundary of the bolt shank is assumed to be connected with spring elements. (See Fig. 3(c).) Rotscher as reported by Wileman et. al.⁽²⁾ first proposed the following equation assuming that the stressed zone is contained within two conical frustra symmetric about the midplane of the joint as shown in Fig. 2.

$$k_m = \frac{\pi E}{4L} \left((d_w + \frac{L}{2})^2 - d^2 \right) \quad (1)$$

where k_m is the combined stiffness of the member, L is the grip length of the joint, d is the bolt diameter, and d_w is the diameter of the washer. Shigley and Mischke⁽⁴⁾ devised the following expression having angle α as a variable.

$$k_m = \frac{\pi E d \tan \alpha}{2 \ln \left\{ \frac{(L \tan \alpha + d_w - d)(d_w + d)}{(L \tan \alpha + d_w + d)(d_w - d)} \right\}} \quad (2)$$

The spring stiffness is assumed to be the stiffness in (2) along the boundary of the bolt shank.

2.1.4. Modelling (d)

The spring elements in Modelling (c) are simply replaced by the rigid elements just to model the bolt shank. (See Fig. 3(d).)

2.1.5. Modelling (e)

The bolted joint has been idealized as 5 eight-noded three-dimensional solid elements (CHEXA elements of NASTRAN) which fill the bolt space^{(5),(6)}. (See Fig. 3(e).) The area of the shaded decagon is identical to the effective cross sectional area of the bolt shank. To match

compatibility of the plate/shell elements (CQUAD4 elements) and the solid elements (CHEXA elements), RBE3 elements of NASTRAN⁽⁷⁾ are used. These are required because plates have 6 degrees of freedom whereas solids have only 3 degrees of freedom.

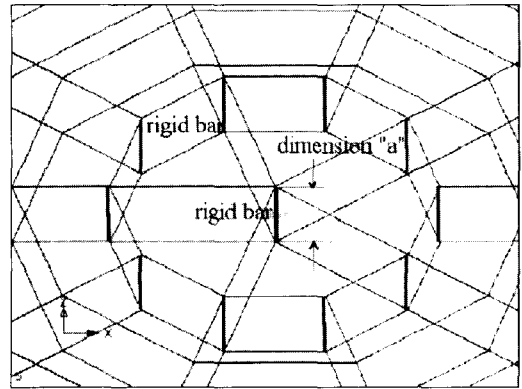


Fig. 3 (d) Modelling (d): Rigid elements at the center and along the boundary of the bolt shank

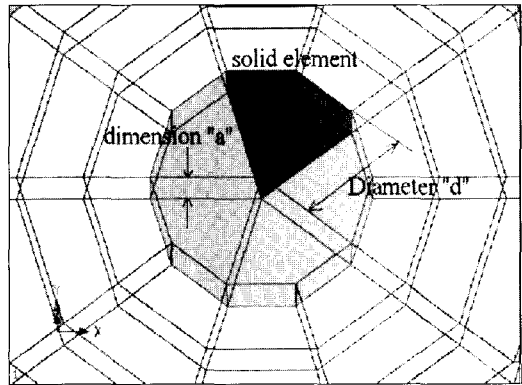


Fig. 3 (e) Modelling (e): Solid elements to fill the bolt space

2.2 Experimental verification

To determine the modelling technique which produces the most satisfactory results, both dynamic and static experiments are conducted for an

experimental model.

2.2.1 Modal experiment

First, modal testing is performed to estimate how well the modelling techniques predict the natural frequencies. Since the first few natural modes are associated with the global behavior of structures, the correct prediction of the first few natural frequencies will be an indication of the proper modelling of the overall structural stiffness. The selected experimental model consists of two plates connected by six bolts as illustrated in Fig. 4. The detailed geometry of this model is shown in Fig. 5. Thirty impact points are selected and each point is excited 5 times for averaging.

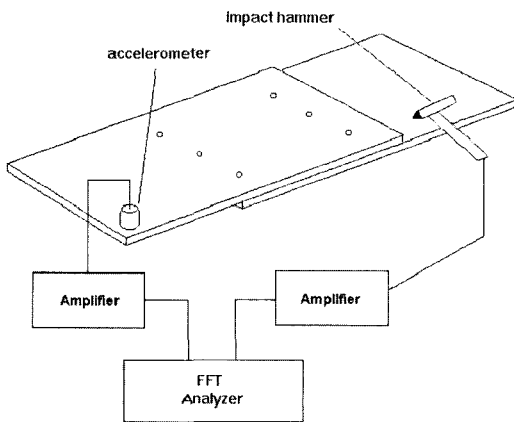


Fig. 4 Dynamic experimental setup for modal analysis

Table 1 shows the natural frequencies obtained by the experiment and various finite element models. It is evident that the calculated frequencies by Modelling (e) show the best agreement with the measured frequencies. Since Modelling (d) using rigid elements overestimates

the stiffness of bolted joints, the calculated frequencies are higher than the experimental frequencies. Fig. 6 shows the modal assurance criterion (MAC) values between the experimentally measured mode shape (f_x) and the numerically calculated mode shape (f_p) from Modelling (e). MAC by Ewins⁽⁸⁾ provides the measure of the least squared deviation of the points from the straight line correlation. Its definition is given by

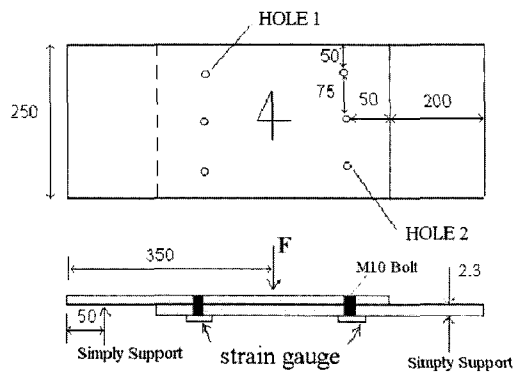


Fig. 5 Geometry of the test model (unit = mm)

$$MAC(p,x) = \frac{|\sum_{j=1}^n (\phi_x)_j (\phi_p)_j^*|^2}{(\sum_{j=1}^n (\phi_x)_j (\phi_x)_j^*) \cdot (\sum_{j=1}^n (\phi_p)_j (\phi_p)_j^*)} \quad (3)$$

Table 1 Natural frequencies obtained from the experiment and the finite element analysis (unit = Hz).

Mode No.	EXP.	Model (a)	Model (b)	Model (c)	Model (d)	Model (e)
1	30.83	28.6	29.1	30.3	31.5	31.0
2	55.94	52.9	53.7	55.2	57.2	56.2
3	58.49	55.9	55.9	59.0	59.6	58.9
4	82.65	80.0	80.3	82.6	83.7	82.7
5	140.1	135.8	137.4	140.4	144.1	142.1
6	155.1	143.1	145.8	148.7	154.5	152.0
7	193.2	175.9	175.9	193.7	197.0	194.8

Fig. 6 exhibits the numerically determined mode shapes from Modelling (e) are noticeably similar to the experimentally determined mode shapes. This resemblance confirms that Modelling (e) is more accurate and efficient in the modal analysis of the structure with bolted joints compared to any other modelling techniques.

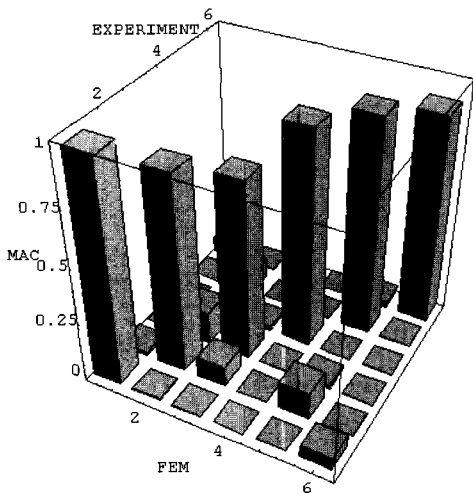


Fig. 6 MAC (Modal Analysis Criteria). FEM indicates the results obtained from modelling technique (e).

2.2.2 Static experiment

A 3-point bending experiment is also executed to investigate the performance of each modelling method in predicting the local stress distribution around the bolted joints. The static experimental setup is presented in Fig. 7. The MM 062RF type 3-element rectangular rosettes are employed to measure strains at the points 4 mm apart from the bolt holes.

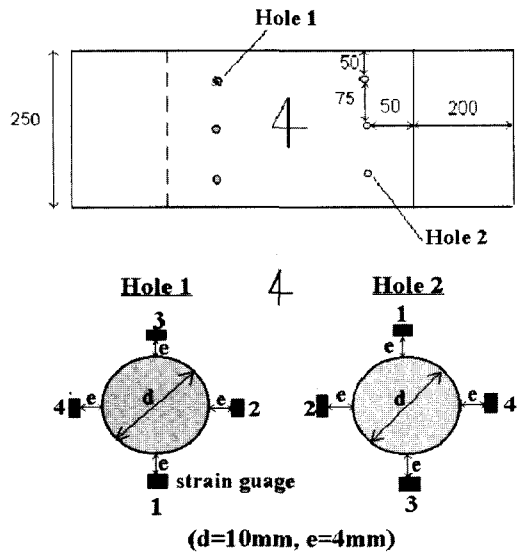


Fig. 7 Static experimental setup

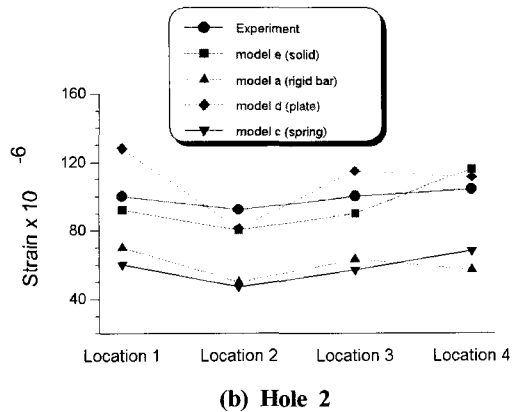
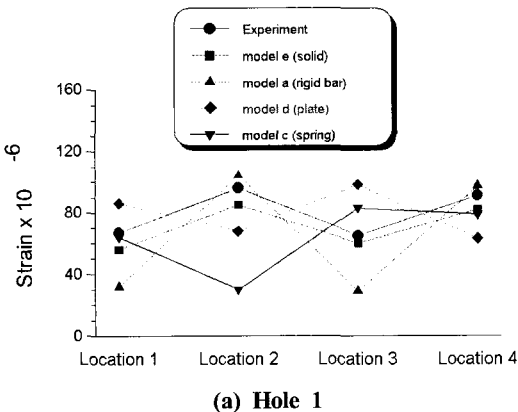


Fig. 8 von-Mises strains (a) around hole 1, and (b) around hole 2. Models (a) through (e) indicate the results from the various finite element modelling techniques.

The experimental and numerical von-Mises strains are compared in Fig. 8. It is apparent that the results from Modelling (e) almost coincide with the experimental results both pattern-wise and magnitude-wise. Similar observations are made for strains near other bolt holes. From the present comparison, Modelling (e) yields the most satisfactory static and dynamic results. Based on this results, domestically-manufactured commercial vehicle frames are to be investigated in the subsequent section.

3. Analysis of the frame with bolted joints

Fig. 9 shows the finite element model of the chassis frame near the trunnion bracket mounting. The flange of the side member and cross member is connected by a gusset plate. Utilizing Modelling technique (e), the bolted joints shown in gray are modeled as 4 solid elements which fill the octagonal space.

The finite element analysis is performed under 3 end load conditions (bending moment, normal force and axial force) as indicated in Fig. 9. In fact, one can roughly estimate the actual magnitude of the in-plane bending moments and normal forces acting on the element of the chassis frames⁽⁹⁾. However, a unit load is used for the sake of simplicity since we are interested in determining key design variables. The bolted joint connects the side member, cross member, gusset plate (stiffener), and trunnion bracket in the vehicle frame in consideration. Accordingly, the finite

element modelling of the chassis frames is assumed to be fixed at the bottom of the bolted joint as it is connected to the trunnion bracket which may be regarded rigid.

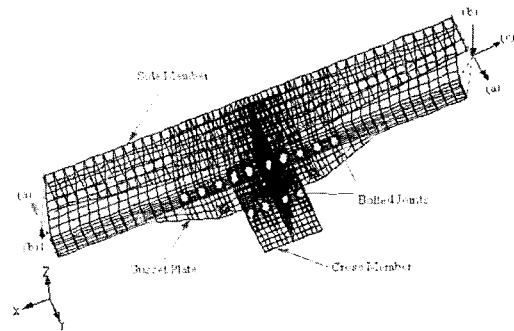


Fig. 9 The finite element modelling of the chassis frame near the trunnion bracket mounting under various load conditions (a) bending moment (b) normal force (c) axial force. The bottom of the bolted joints is assumed to be fixed.

Using the geometry given for Model A in Table 2, the finite element analysis with the above-mentioned boundary condition is carried out. To identify the key design variables, we consider several different models, some of which are described in Table 2 and Fig. 10. It should be noted that crack problems have been reported more frequently near the bolted joints of the gusset plate of Model A than Model B and C. For different loading conditions, the maximum stresses relative to the maximum stress of Model A are plotted in Fig. 11. The magnitudes of the torsional and bending rigidities of different models are also shown in Fig. 11. It is worth noting the maximum stress is governed mainly by the torsional rigidity in all loading conditions. Even

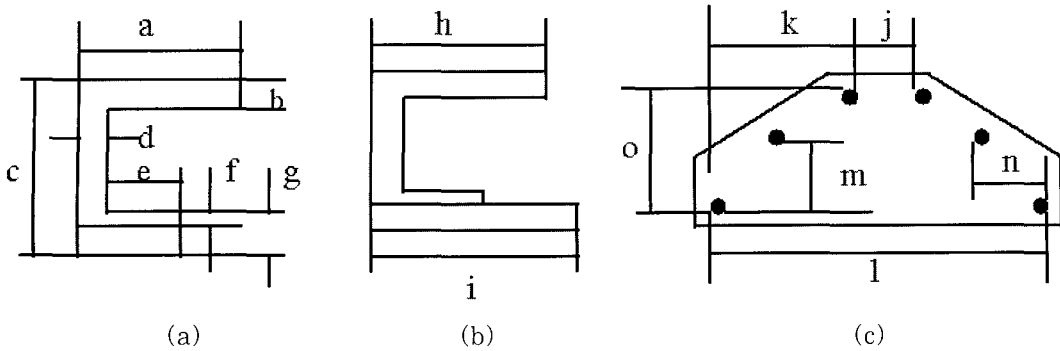


Fig. 10 The geometries of the frame cross sections and the trunnion bracket. (a) The cross section of the frame where the loads act, (b) the cross section of the frame just in front of the bolted joint where the maximum stress is known to occur, and (c) the plane figure of the trunnion bracket

when a bending moment is applied at one end, significant twisting deformations have been observed. Thin-walled open beams have outstanding resistance to bending but poor resistance to twisting. From these and other results, the torsional rigidity is obviously a far more important design variable than the bending rigidity in the present frame as it is composed of thin-walled open beams. Once vehicles are actually being manufactured, the frame geometry change

is not a trivial matter. Thus one may consider other alternatives, such as the change of the gusset plate thickness or the trunnion bracket dimensions indicated by *j*, *k*, *l*, *m*, and *o* in Fig. 11.

Table 2 Dimensions of three models in Figure 10 (unit=mm)

Variables	Model A	Model B	Model C
a	156.3	160	160
b	23	25	30
c	328	324	324
d	15	13	8
e	82.5	95	98
f	15	19	14
g	23	31	25
h	235.5	238	230
i	152.5	140.8	161.8
j	200	140	260
k	205	240	220
l	610	620	700
m	100	80	110
n	125	90	70
o	190	205	195

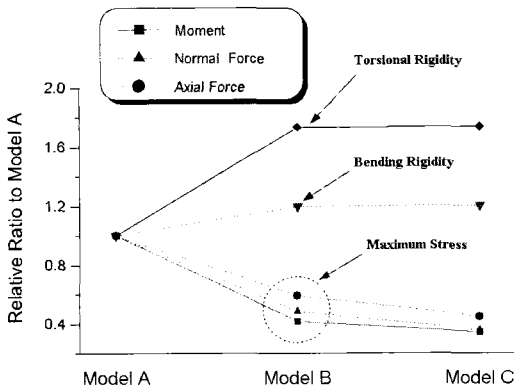


Fig. 11 The relation between the sectional properties and the maximum principal stress

3.1 Gusset plate thickness change

To examine the effect of the gusset plate thickness change, the thickness t is varied from 8 to 16 mm in Model A. Fig. 12 shows the maximum principal stress and frame sectional properties for different values of the thickness. As expected, the maximum principal stress diminishes as the thickness of the gusset plate increases. However, it is imperative to realize decrease of the maximum principal stress is almost proportional to increase of the torsional rigidity. Specifically, as the thickness t varies from 8 to 16 mm, the torsional rigidity increases by 34% and the maximum principal stress decreases by 33%. Thus, this numerical experiment demonstrates that thickness of the gusset plate is the most convenient solution to solve the crack problems near the bolted joints.

3.2 Trunnion bracket dimension change

We have also examined the effect of the change of the various bracket dimensions. Among the various dimensions, dimension l , the length between the end bolts of the trunnion mounting, is found to be the most critical design variable. Fig. 13 indicates the maximum stress level is considerably sensitive to dimension l . When l is increased by 2%, i.e., 470 mm to 480 mm, the stress is reduced by up to 7%. Therefore, if a substantial change of the frame section dimension is not tolerated, revising the design of the trunnion bracket with the optimal value of l appears to be a practical alternative in the automotive industry.

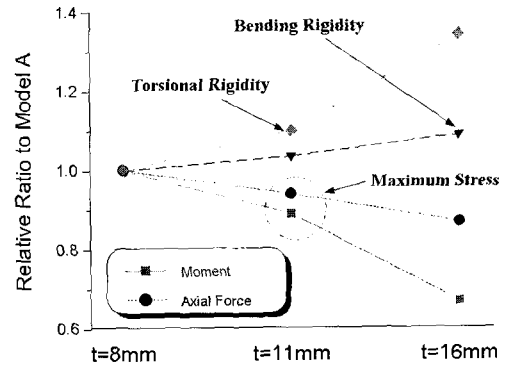


Fig. 12 The relation between the thickness of the gusset plate and maximum principal stress when the frame is under load condition (a) and (c)

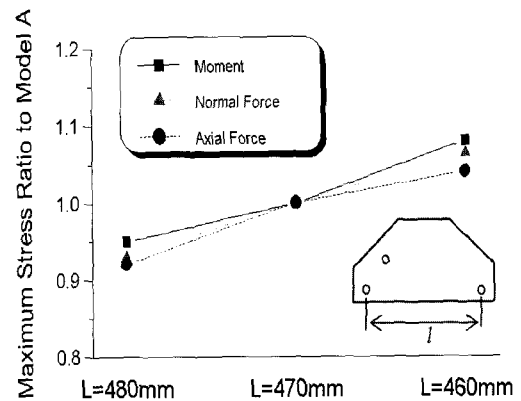


Fig. 13 The relation between the length l of the trunnion bracket and the maximum principal stress

4. Conclusions

Among several bolted joint modelling techniques, the technique to model the bolt with solid elements and the frames with plate/shell elements is shown to be a practically simple, yet reliable technique. Utilizing this technique, the finite element analysis of the vehicle chassis frame near the trunnion bracket was carried out. The numerical

experiments concluded the key design variables are the torsional rigidity of the chassis frame and the trunnion bracket shape. If the frame change is not feasible, adjustment of the distance between the end bolts of the trunnion bracket is a promising alternative for redesigning.

References

- [1] M. Tanaka, H. Miyazawa, E. Asaba and K. Hongo, "Application of the Finite Element Method to Bolt-Nut Joints-Fundamental Studies on Analysis of Bolt-nut Joints Using the Finite Element Method", Bulletin of JSME, Vol. 24, No. 192, pp. 1064-1071, 1981.
- [2] J. Wileman, M. Choudhury and I. Green, "Computation of Member Stiffness in Bolted Connections", ASME Journal of Mechanical Design, Vol. 113, pp. 432-437, 1991.
- [3] J. Kim, S. Park, Y. Kim, S. Choi, B. Kim, "Finite Element Modelling and Experimental Verification of the Structures with Bolted Joints", J. of KSME, A, Vol. 20, No. 6, pp. 1854-1861, 1996.
- [4] J. E. Shigley and C. R. Mischke, Mechanical Engineering Design, Fifth Edition, New York, McGraw-Hill, 1989.
- [5] H. J. Beermann, "Static Analysis of Commercial Vehicle Frames: A Hybrid-Finite Element and Analytical-Method", Int. J. Vehicle Des., Vol. 5, pp. 26-52, 1984.
- [6] L. Garro, and V. Vullo, "Deformations Car Body Joints Under Operating Conditions", SAE 861397, 1986.
- [7] M. Reymond and M. Miller, MSC/ NASTRAN Quick Reference Guide, Los Angeles, The Macneal-Schwendler Corp., Ver. 68, 1994.
- [8] D. J. Ewins, Modal Testing: Theory and Practice, Letchworth, England, Research Studies Press Ltd, 1984.
- [9] H. J. Beermann, The Analysis of Commercial Vehicle Structures, London, Mech. Eng. Publication Limited, 1989.

저 자 소 개



김진곤 (金辰坤)

1967년 11월생, 1991년 서울대학교 기계설계학과 졸업, 1993년 서울대학교 기계설계학과 석사, 1998년 서울대학교 기계설계학과 박사, 1998-2000 삼성전자, 2001년~현재 대구가톨릭대학교 기계자동차공학부 조교수.



박용국 (朴鏞國)

1964년 11월생, 1987년 서울대학교 공학사, 1989년 University of Michigan (공학석사), 1995년 Ohio State University (공학박사), 1996년 Ohio State University(Post-Doctoral), 1996-1998년 삼성자동차 금형기술연구소, 1998~현재 대구가톨릭대학교 기계자동차공학부 부교수.